NASA TECHNICAL MEMORANDUM

NASA TM X-1606

NASA TM X-1606

REDUCTION OF WIND-TUNNEL-MODEL VIBRATION BY MEANS OF A TUNED DAMPED VIBRATION ABSORBER INSTALLED IN THE MODEL

by William B. Igoe and Francis J. Capone

Langley Research Center
Langley Station, Hampton, Va.

NATIONAL AERONAUTICS AND SPACE ADMINISTRATION • WASHINGTON, D. C. • JULY 1968

NASA TM X-1606

REDUCTION OF WIND-TUNNEL-MODEL VIBRATION BY MEANS OF A TUNED DAMPED VIBRATION ABSORBER INSTALLED IN THE MODEL

By William B. Igoe and Francis J. Capone

Langley Research Center
Langley Station, Hampton, Va.

NATIONAL AERONAUTICS AND SPACE ADMINISTRATION

For sale by the Clearinghouse for Federal Scientific and Technical Information
Springfield, Virginia 22151 – CFSTI price $3.00

REDUCTION OF WIND-TUNNEL-MODEL VIBRATION BY MEANS OF A TUNED DAMPED VIBRATION ABSORBER INSTALLED IN THE MODEL

By William B. Igoe and Francis J. Capone
Langley Research Center

SUMMARY

Some experimentally determined performance characteristics have been presented for a tuned damped vibration absorber which was designed to reduce the undesirable rigid-body vibrations of a conventional wind-tunnel force model. The model vibration was due to random excitation by wind-tunnel airstream turbulence and buffeting. A tuned vibration absorber was used for this purpose because it was compact and did not require any force linkages across the force balance.

The absorber was tuned to reduce vibrations in both the pitch and yaw planes simultaneously, but its effectiveness in yaw was restricted because the mass center of the absorber was near the node of the yaw vibration mode. In the pitch plane, the peak and root-mean-square amplitudes of the rear normal-force-component fluctuations of the balance were reduced by approximately 50 percent at some wind-tunnel test conditions.

INTRODUCTION

The presence of excessive model vibrations during steady-state wind-tunnel force tests is generally undesirable because of possible interference with the achievement of the primary objectives of the test. For example, dynamic stresses caused by vibration may approach the structural static or fatigue stress limits of the model or its support system and restrict the allowable range of test variables. A more serious vibration problem may be the existence of unsteady forces or displacements which cannot be satisfactorily time-averaged for steady-state results.

An instance of the latter effect of model vibration was encountered in the Langley 16-foot transonic tunnel during conventional wind-tunnel force tests of a 1/20-scale model of a multimission variable-sweep fighter airplane. The model was mounted on a six-component internal strain-gage force balance and was sting supported from the rear. Under wind-on conditions, random model vibrations, induced by wind-tunnel airstream turbulence and buffeting, caused intermittent dynamic fouling to occur between the base of the model and the sting support. As indicated by the balance, the time average of the axial force was affected by the fouling, which resulted in an error in that component.

One of the steps taken to solve the fouling problem was to design a tuned damped vibration absorber to reduce the amplitude of vibration of the model. The use of a tuned absorber to reduce random dynamic response is not new. For example, reference 1 describes the performance of two tuned absorbers, one in each wing tip of a Lockheed F-80A airplane, where the absorbers were tuned to reduce the airplane buffeting response in flight in the wing second antisymmetric bending mode.

For the wind-tunnel tests of the present study, the choice of a vibration absorber as a vibration-reduction device was influenced primarily by the requirement that the device not exert any forces across the force balance. In addition, the device had to be compact because of space limitations inside the model. The tuned damped vibration absorber which is described in reference 2 satisfied these conditions.

The vibration absorber has certain disadvantages which limit its effectiveness. In its simplest form, it can be tuned to absorb only one mode of vibration. A complex vibrating system such as a wind-tunnel model can have several significant modes of vibration. The absorber effectiveness is also very dependent on accurate tuning. For a wind-tunnel model, this tuning often cannot be accomplished simultaneously for all test conditions because the response frequency of the model may be a function of the Mach number and dynamic pressure of the test. An added disadvantage is that the absorber reduces the model response with respect to an inertial frame of reference instead of with respect to the sting which supports the force balance. The sting support is itself a flexible structure, subject to vibratory response as part of the model dynamic system.

The purpose of this report is to present some performance characteristics of the wind-tunnel-model tuned damped vibration absorber. In the wind-tunnel tests, the model response was measured with and without the absorber installed, at Mach numbers from 0.44 to 1.26. Bench tests were also conducted on a model simulator to determine some of the absorber frequency-response characteristics.

APPARATUS AND PROCEDURE

Tuned Damped Vibration Absorber

As described in reference 2, the tuned vibration absorber is an additional (spring-mass) single-degree-of-freedom system which is attached to the mass of the main (spring-mass) single-degree-of-freedom system whose vibrations are to be reduced, to create a coupled two-degree-of-freedom system. If the excitation of the main system is harmonic at a constant discrete frequency, then for optimum performance, the natural frequency of the absorber is made equal to the excitation frequency. If the excitation frequency is not constant, then for optimum performance, damping must be introduced to the absorber, and its natural frequency must be made equal to the main-system natural frequency divided by (1 + mass ratio). The mass ratio is the ratio of the absorber mass to the main-system mass. Reference 2 shows that optimum damping varies from about 12 percent to 24 percent of critical damping for mass ratios from 0.05 to 0.50. Critical damping is the minimum amount of damping required to prevent overshoot of a dynamic system as it returns to equilibrium.

If the main dynamic system is one with several degrees of freedom or is an elastic structure with distributed mass, it can have several significant modes of vibration. For such systems, the vibration absorber can be tuned to reduce the response in a particular mode of vibration, and the admittance of the system is thus correspondingly modified. The admittance of a dynamic system is the response of the system to a harmonic excitation of constant unit amplitude as a function of frequency.

The performance characteristics of the absorber, in combination with a dynamic system having one or more degrees of freedom or normal modes of response and being subjected to a stationary random excitation, may be obtained by means of the techniques of generalized harmonic analysis. A descriptive review of these techniques and their application is presented in reference 3. The power spectral density of the response at any frequency is equal to the product of the power spectral density of the excitation and the square of the amplitude of the admittance at that frequency. The mean-square amplitude of the response may be obtained by integrating the power spectral density with respect to frequency from zero to infinity. The root-mean-square amplitude is a measure of the time average of the random amplitude of the response. Dynamic systems with rotational degrees of freedom are of course conceptually analogous to systems with translational degrees of freedom.

The absorber used in the present tests is shown in the sketch of figure 1 and the photographs of figure 2. It had a shaped mass, suspended on a steel cantilever spring and enclosed in an aluminum case filled with damping fluid. The absorber mass consisted of a 2.68-kilogram block of tungsten alloy. The irregular shape of the absorber was necessitated by its adaptation to limited space and existing model contours.

Tuning was accomplished by varying the spring cross-sectional dimensions, spring length, and mass location. The dimensions of the steel cantilever spring were chosen to provide specific frequencies in both the pitch and yaw planes simultaneously. The spring cross section was rectangular, with depth and width dimensions approximately in the same ratio as the desired pitch and yaw frequencies. Some of the absorber spring and mass dimensions are presented in figure 3. The absorber mass position could be changed about 0.25 centimeter longitudinally on the spring. Three different sets of spring cross-sectional dimensions are shown in the table of figure 3, although only spring 3 was used in the wind-tunnel tests. The table also includes the resonant frequencies of the absorber in both pitch and yaw for the three spring sizes with different spring lengths and mass positions.

The thin-walled aluminum case was shaped to enclose the absorber mass with an internal clearance of about 0.6 centimeter. For the wind-tunnel tests, the damping fluid used was silicone oil with a nominal kinematic viscosity of 350 centistokes $\left(3.5 \times 10^{-4}\ m^2/sec\right)$ at a temperature of about 298° K; however, fluids of other viscosities were used for the bench tests.

Model Simulator

Several characteristics of the absorber-model system were difficult to determine analytically. Among these were the viscosity of the fluid required for optimum damping, the apparent increase in the absorber mass due to its vibration and the consequent induced motion of the surrounding fluid in the container, and the effective mass ratio of the absorber-model system. To determine these characteristics experimentally, bench tests were performed. A dynamic simulator, shown in the sketch of figure 4 and the photograph of figure 5, was weighted to correspond approximately to the model with respect to mass, mass balance, and moment of inertia. The simulator was suspended from a short cantilever spring located at the node and could be tuned to the model wind-on frequency to simulate the model rigid-body pitch or yaw vibration modes.

Wind-Tunnel Model

The wind-tunnel tests were conducted on a 1/20-scale model of a multimission tactical fighter airplane with variable-sweep wings, as shown in the sketch of figure 6. The sweep of the outboard wing panels was 72.5° for the present tests. The model, which had a mass of about 31.7 kilograms and a mass center located about 67 centimeters behind the nose, was mounted on a six-component internal strain-gage force balance and was sting supported from the rear. Some of its dynamic characteristics are presented in table I. A complete description of the geometrical characteristics of the model is presented in reference 4 (land-based configuration).

Instrumentation

The six-component, strain-gage force balance was a cylindrical balance of the floating-frame type. The instrumentation used to determine the wind-off frequency characteristics of the absorber, model simulator, and model is shown in the block diagram of figure 7(a). The amplitude of vibration was obtained from the accelerometer output by dividing by the square of the frequency. A block diagram for the instrumentation used to record data during the wind-tunnel tests is shown in figure 7(b). The fluctuating component of the balance output was recorded on a 14-channel magnetic tape recorder utilizing a frequency-modulation (FM) system. The tape records were analyzed for root-mean-square-amplitude and power-spectral-density information on analog data-reduction equipment similar to that which is described in reference 5.

TABLE I.- WIND-OFF RIGID-BODY MODEL CHARACTERISTICS

[Balance moment center 62.1 cm behind model nose]

Vibration mode	Resonant frequency, hertz	Location of node, cm (a)
Sting yaw	6.2	109
Balance yaw	13.9	61
Balance yaw	21.9	43
Sting pitch	8.7	---
Balance pitch	26.4	48

Configuration	Mass, kg	Mass center, cm (a)
Absorber (assembled)	3.27	38
Model	31.7	67

[a]Measured from model nose.

Wind Tunnel

The wind-tunnel tests were conducted in the Langley 16-foot transonic tunnel. It is a closed-return wind tunnel having a slotted octagonal test section and operating at atmospheric stagnation pressure at Mach numbers from 0.2 to 1.3. Reference 6 contains a description of the tunnel and its main drive system for Mach numbers below 1.1. Currently, the Langley 16-foot transonic tunnel utilizes auxiliary plenum suction for Mach numbers from 1.1 to 1.3.

Tests

The bench tests consisted of measuring the resonant frequencies of the absorber spring-mass system, which are listed in figure 3, and determining the frequency-response characteristics of the model simulator in combination with the absorber. For part of the latter tests, the simulator was tuned to a resonant frequency of 20.1 hertz, and the mass center of the absorber was located about 18 centimeters from the simulator cantilever spring mounting. The simulator was then tuned to a model wind-on yaw frequency of 22.5 hertz with the absorber mass center located 18 centimeters and 5 centimeters from the cantilever spring. Finally, a model wind-on pitch frequency of 25.4 hertz was simulated, with the absorber mass center located 18 centimeters from the spring.

During the wind-tunnel tests, the absorber was positioned in the model as shown in figure 6. Magnetic-tape and oscillograph records were taken with the model nominally at zero angle of attack at Mach numbers from 0.44 to 1.26, with and without the absorber installed. Oscillograph records were also taken at the maximum angles of attack, which varied from about 5° to 7°, depending on the Mach number. The model dynamic-response characteristics at those angles were not substantially different from the response characteristics at zero angle of attack and, consequently, only the data for zero angle of attack are presented. The root-mean-square amplitudes were obtained directly from analysis of the magnetic-tape records. To determine the power-spectral-density distributions, transcribed loops representing time samples of 30 seconds were analyzed with a 1-hertz bandwidth filter. The force-balance output was not calibrated on the magnetic-tape recorder during the wind-tunnel tests. As a result, the root-mean-square and power-spectral-density analyses of the balance components are known only in relative proportion with respect to each other, rather than in absolute magnitude.

The wind-off resonant frequencies of the model were obtained in the wind tunnel by means of instrumentation as shown in figure 7(a) for the bench tests. The significant rigid-body pitch and yaw frequencies of the model are presented in table I.

RESULTS AND DISCUSSION

Bench Tests on Model Simulator

As mentioned previously, the primary purpose of the bench tests on the model simulator was to measure certain characteristics of the absorber-model system which were difficult to calculate. These characteristics were the effective mass ratio of the absorber-model system, the effects of apparent additional mass, and the viscosity of the fluid required for optimum damping. The simulator also provided a means of tuning the absorber for a measured wind-on model frequency with the relative convenience of bench tests. Actually, the effective mass ratio need not be known when the absorber tuning is accomplished in this way.

In order to determine the effects of apparent additional mass and the viscosity of the fluid required for optimum damping, the frequency-response characteristics of the simulator in combination with the absorber were determined with fluids of different viscosities as shown in figure 8. The effect of infinitely large viscosity was simulated by blocking the absorber mass so it could not vibrate. Responses were obtained for the absorber with silicone oils having kinematic viscosities of 1762 centistokes and 350 centistokes, and with water having a kinematic viscosity of 1 centistoke, as well as with no damping liquid. The silicone oils had approximately the same density as the water; thus, both liquids produced about the same apparent-additional-mass effect.

A comparison of the frequency-response curves for the absorbers with water and with no damping liquid in figure 8 shows the apparent-additional-mass effect. The presence of two large peaks in both curves shows that the absorber is lightly damped, but with water as the damping fluid, the curve is displaced to lower frequencies because of the apparent increase of the absorber mass.

The curves for the various damping fluids tend to have two common crossing points (labeled P and Q) on the curve for the blocked absorber. Reference 2 shows that the absorber tuning is optimum when the points P and Q have the same displacement amplitude. The curves of figure 8 show that, in this instance, the absorber is tuned to too low a frequency. Optimum damping is indicated when the curves pass through the points P or Q with zero slope. The 350-centistoke-oil curve is seen to peak through the point Q, which indicates that this oil viscosity is near optimum. Near-optimum tuning is shown for the 350-centistoke oil by its curve in figure 9.

From the data of figure 8 and the tabulated frequencies in figure 3, it has been estimated that the absorber-simulator system had an effective mass ratio of about 0.02, and that the apparent increase of the absorber mass was equal to about 0.4 of the mass of the displaced damping fluid.

During the wind-tunnel tests, the silicone oil would be subjected to a varying-temperature environment. The decrease of viscosity with increased temperature is less for silicone oils than for ordinary hydrocarbon oils; however, some loss in damping occurs with increase in temperature. The effect of oil temperature change on the absorber characteristics is shown in figure 10. Temperatures of 297° K and 322° K approximate the temperature limits encountered during the wind-tunnel tests. Figure 10 shows that, for the nominal 350-centistoke oil at a temperature of 297° K, the viscosity is too high for optimum damping (indicated by the single peak between the points P and Q), and that at 322° K, it is too low (indicated by the double peaks outside the points P and Q). (See ref. 2.) At 322° K, the oil viscosity was approximately 200 centistokes.

Figures 11 and 12 present the performance of the absorber with the model simulator tuned to a wind-on frequency of 22.5 hertz in yaw. Figure 11 shows the frequency-response curves with the absorber mass center positioned about 18 centimeters from the effective node. Neither the absorber tuning nor the damping is optimum in this figure. The dependence of the frequency-response characteristics on the position of the absorber with respect to the effective node location is shown in figure 12 in a comparison of the 18-centimeter position with the 5-centimeter position. With its mass center positioned

5 centimeters from the node, the absorber was almost totally ineffective. The frequency-response curves for a simulator wind-on pitch frequency of 25.4 hertz with the absorber positioned 18 centimeters from the effective node are presented in figure 13. Here again, neither the absorber tuning nor the damping is optimum.

Wind-Tunnel Tests on Model

The 1/20-scale variable-sweep fighter model was designed primarily for purposes of determining minimum drag. The afterbody lines of the model were made to correspond as closely as possible to those of the airplane and resulted in a narrow opening at the base of the model through which the sting support could pass. (See fig. 6.) The side clearance between the model base and the sting was of the order of 1 millimeter. During the initial phase of the wind-tunnel force tests, the turbulence level of the tunnel and the buffeting characteristics of the model induced vibrations of sufficient amplitude to cause dynamic fouling in yaw at the model base. Some slight eccentricity of the model base with respect to the sting caused the fouling to occur first on the left side of the model. The force balance in use at the time was a compound type and proved sensitive to the dynamic fouling so that the time average of the axial component was reduced, which resulted in an error in that component. Using a stiffer sting support and a floating-frame-type cylindrical balance in repeating the tests reduced the severity of the dynamic fouling so that the force balance components were not affected by it. The force-data results of the latter tests are reported in reference 4.

Absorber performance in yaw.- During part of the repeat tests, the vibration absorber was installed in the model. The tests without the absorber installed indicated that the yaw vibration mode with a wind-off frequency of 21.9 hertz, as shown in table I, and with a wind-on frequency of about 22.5 hertz, as shown in figure 14, was probably the vibration mode most responsible for the fouling in yaw.

The absorber was therefore tuned (spring 3) for a wind-on yaw frequency of 22.5 hertz, which occurred at a Mach number of 1.16. Table I shows that under wind-off conditions, the yaw node for this vibration mode (21.9 hertz) was located about 5 centimeters behind the mass center of the absorber, which resulted in a very short moment arm through which the absorber could act. The performance of the absorber is dependent on the length of the moment arm since it affects the effective mass ratio and the vibration amplitude through which the absorber is excited.

The root-mean-square amplitudes of the balance force components are shown in figure 15 as functions of Mach number. The front and rear side-force components show that the absorber was relatively ineffective in yaw. A reduction of about 15 percent was obtained on the rear side-force component at a Mach number of 1.16. The spectra of the rear side force at a Mach number of 1.16, presented in figure 14, show some effectiveness of the absorber at the frequency of 22.5 hertz for which it was tuned, and additional reduction at a frequency of about 26.5 hertz. The peak in the yaw spectra at this frequency was caused by a feed-through of the pitch vibration onto the side-force gages. Since the pitch response at 26.5 hertz was reduced by the absorber, this peak on the side-force spectra was similarly reduced.

Absorber performance in pitch.- With the absorber tuned for the yaw vibration mode, the cross-sectional geometry of the absorber cantilever spring determined the pitch tuning. For the pitch vibration mode, table I shows that the absorber mass center was about 10 centimeters ahead of the pitch node. The root-mean-square amplitudes of the front and rear normal-force components shown in figure 15 indicate that the absorber was, in general, more effective in pitch than it was in yaw. At a Mach number of 0.945, the amplitude of the rear normal-force component was reduced by approximately 50 percent.

Figure 16 shows a comparison of the power spectral densities of the front and rear normal-force components for the model with and without the absorber at Mach numbers from 0.915 to 0.965. The reductions in power occur primarily in the peaks at 26.5 hertz. At some frequencies, particularly for the sting pitch vibration mode at 8 hertz in the front normal-force spectrum, the power spectral density was increased slightly with the absorber installed. Because of noise levels present in both the recording and analyzing equipment, the power spectral densities of figures 14 and 16 are probably valid only over a range of about 15 decibels or about 1.5 cycles on the log scale down from the peak values for each spectrum.

A 1.2-second sample of the time-history oscillograph traces for the six balance components is presented in figure 17 for a Mach number of 0.945. The peak-to-peak reduction in the normal-force traces is comparable to that shown for the root-mean-square amplitudes in figure 15. The increase in axial response at this Mach number is caused by the addition of the deadweight mass of the absorber (inert in the axial direction), which lowered the axial response frequency to nearly an integral multiple (third harmonic) of the 26.5-hertz pitch frequency.

CONCLUDING REMARKS

Some experimentally determined performance characteristics have been presented for a tuned damped vibration absorber which was designed to reduce the undesirable rigid-body vibrations of a conventional wind-tunnel force model. The model vibration was due to random excitation by wind-tunnel airstream turbulence and buffeting. A tuned vibration absorber was used for this purpose because it was compact and did not require any force linkages across the force balance.

The absorber was tuned to reduce vibrations in both the pitch and yaw planes simultaneously, but its effectiveness in yaw was restricted because the mass center of the absorber was near the node of the yaw vibration mode. In the pitch plane, the peak and root-mean-square amplitudes of the rear normal-force-component fluctuations of the balance were reduced by approximately 50 percent at some wind-tunnel test conditions.

Langley Research Center,
National Aeronautics and Space Administration,
Langley Station, Hampton, Va., February 26, 1968,
126-13-02-20-23.

REFERENCES

1. Thompson, Jim Rogers; and Yeates, John E., Jr.: A Limited Flight Investigation of the Effect of Dynamic Vibration Absorbers on the Response of an Airplane Structure During Buffeting. NACA RM L54K02, 1955.

2. Den Hartog, J. P.: Mechanical Vibrations. Fourth ed., McGraw-Hill Book Co., Inc., 1956, pp. 87-106.

3. Press, Harry; and Houbolt, John C.: Some Applications of Generalized Harmonic Analysis to Gust Loads on Airplanes. J. Aeronaut. Sci., vol. 22, no. 1, Jan. 1955, pp. 17-26, 60.

4. Re, Richard J.: Transonic Longitudinal Aerodynamic Characteristics of a Variable-Sweep Tactical Fighter Model With Wing Sweeps of 26° and 72.5°. NASA TM X-1259, 1966.

5. Smith, Francis B.: Analog Equipment for Processing Randomly Fluctuating Data. Aeron. Eng. Rev., vol. 14, no. 5, May 1955, 113-119.

6. Ward, Vernon G.; Whitcomb, Charles F.; and Pearson, Merwin D.: Air-Flow and Power Characteristics of the Langley 16-Foot Transonic Tunnel With Slotted Test Section. NACA RM L52E01, 1952.

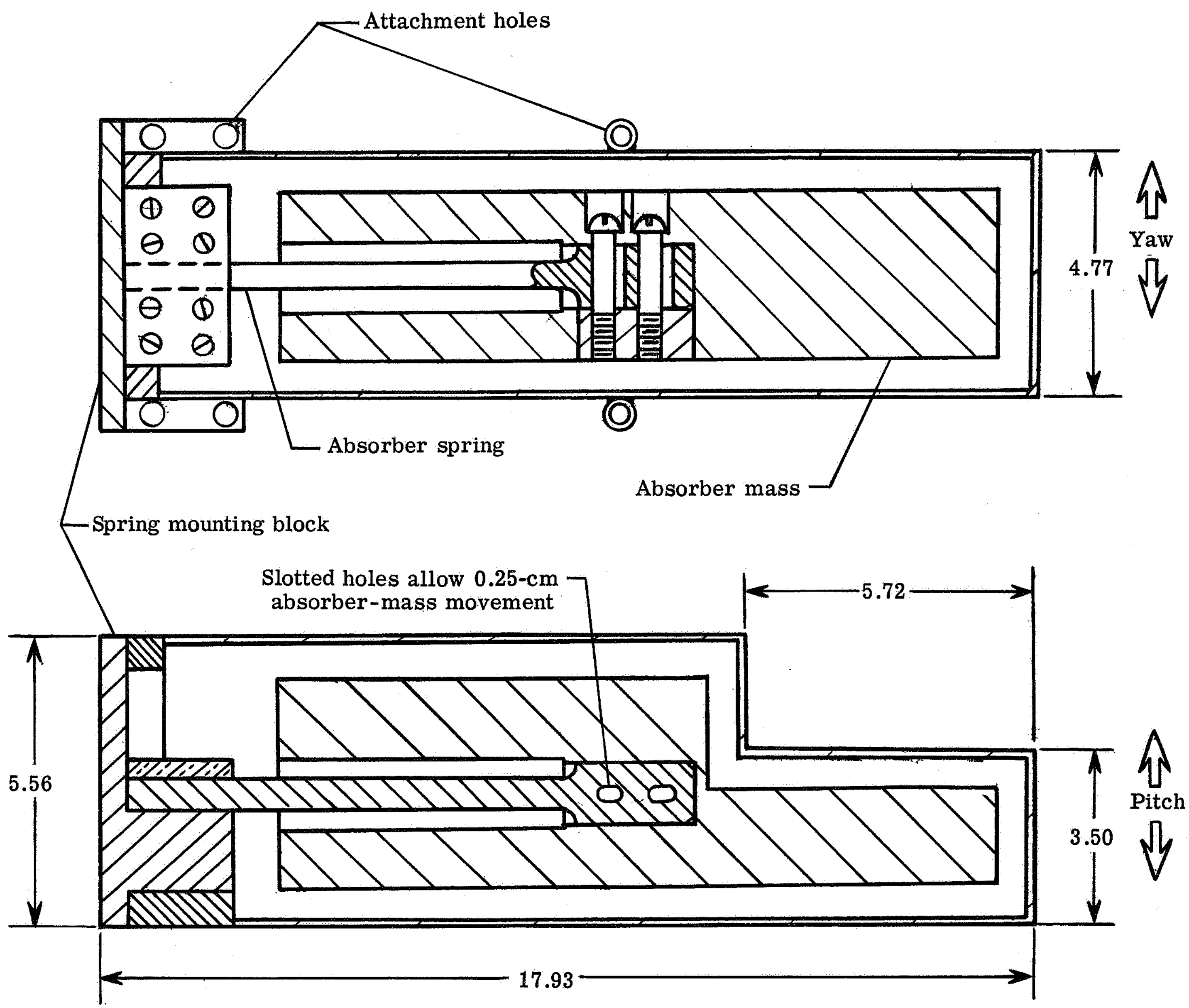

Figure 1.- Sketch of assembled vibration absorber. All dimensions are in centimeters.

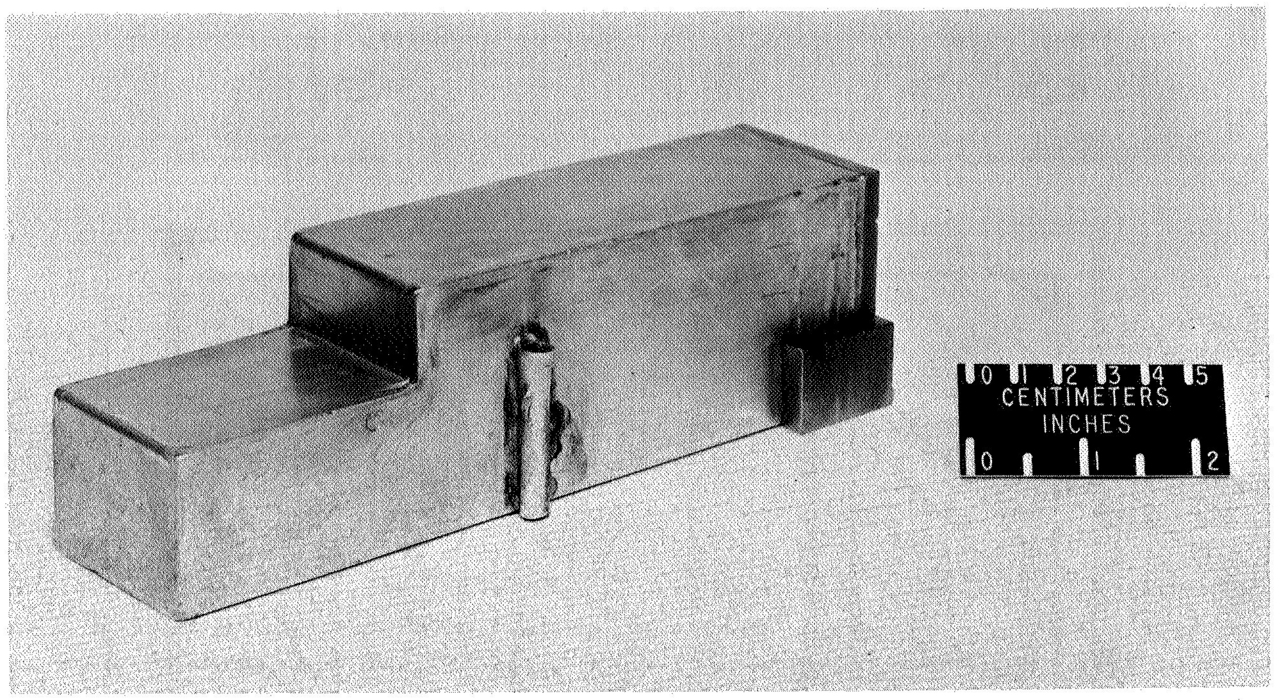

(a) Assembled vibration absorber. L-66-10061

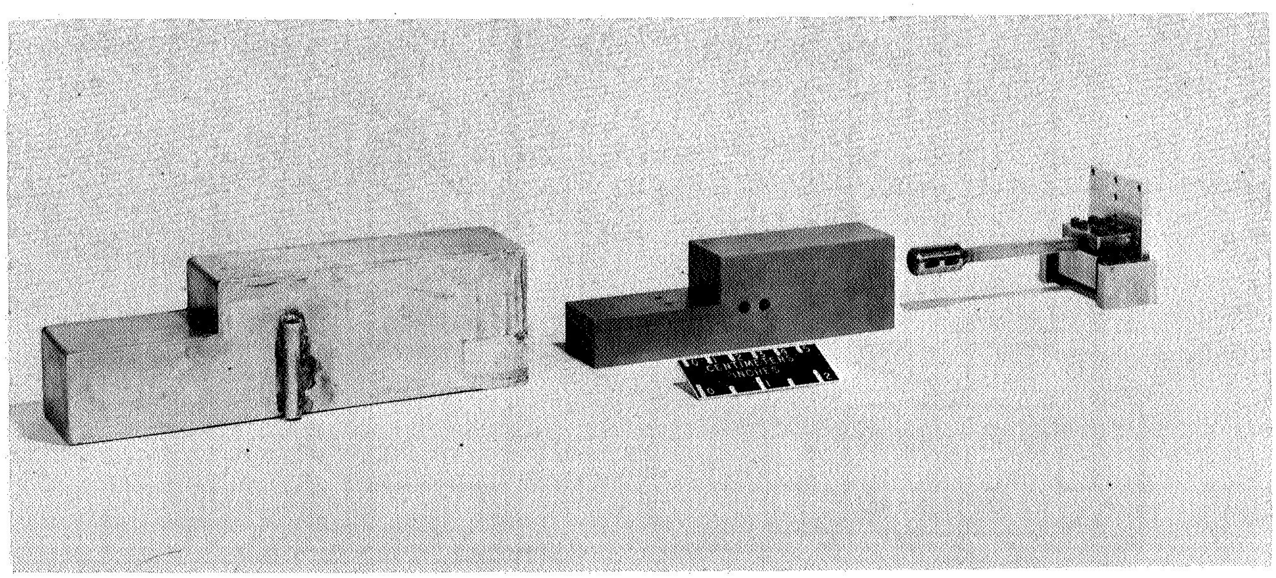

(b) Disassembled vibration absorber. L-66-10062

Figure 2.- Photographs of vibration absorber.

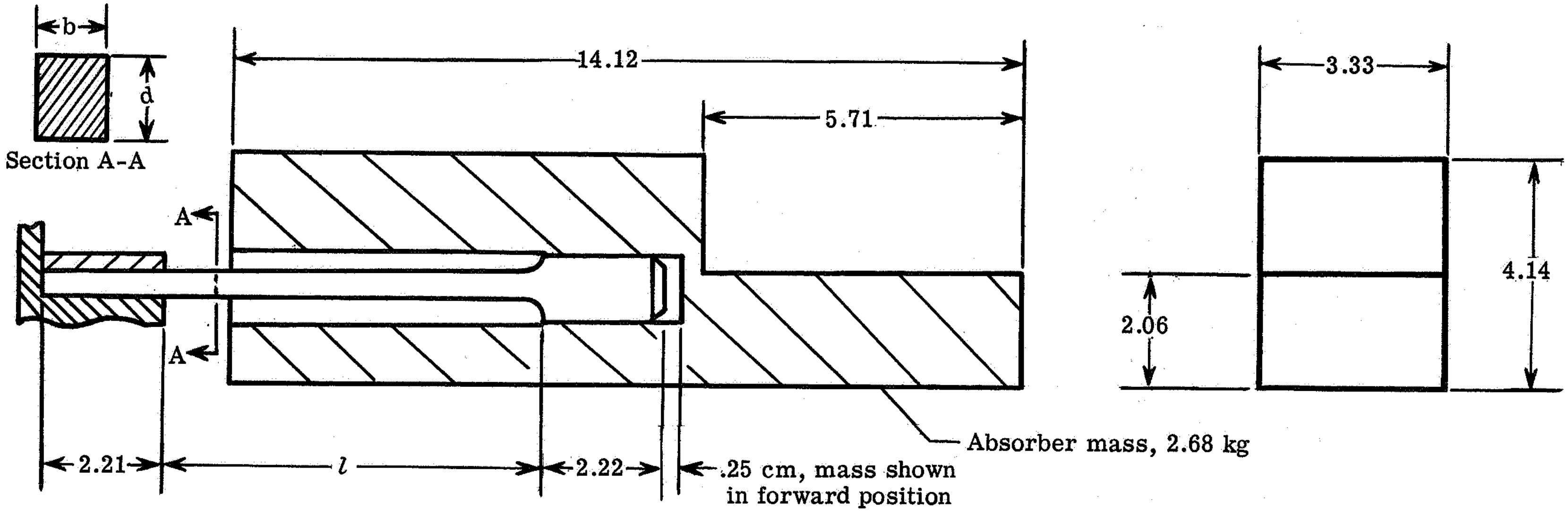

Spring	l	b	d	Yaw frequency, hertz	Pitch frequency, hertz	Mass position
1	6.109	0.457	0.523	20.55	23.14	Aft
2	6.634	.472	.544	21.06	23.78	Aft
3	6.563	.508	.582	23.66	25.57	Midway
4	6.563	.508	.582	24.04	26.07	Aft

Figure 3.- Sketch showing spring and mass details. All dimensions are in centimeters except where noted.

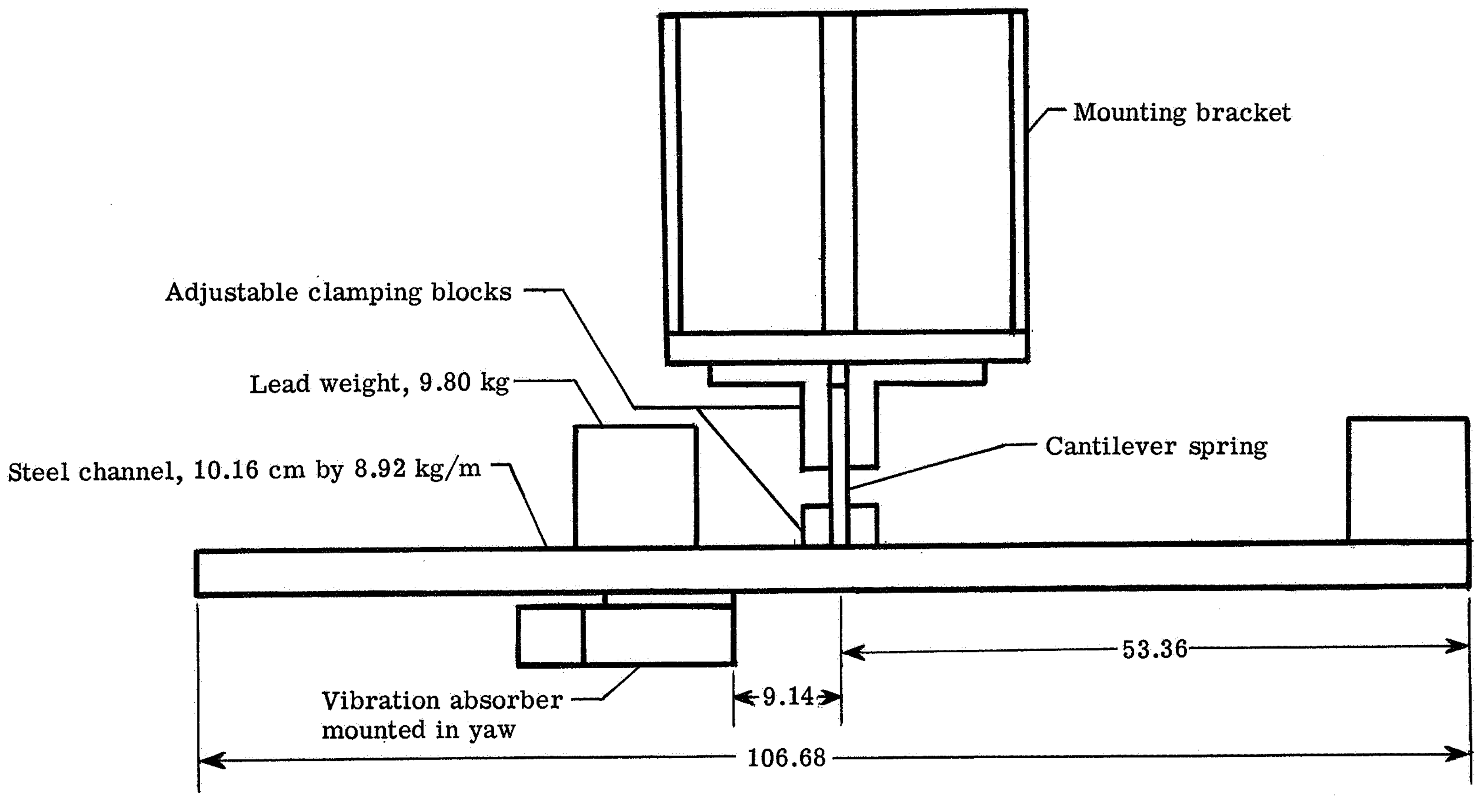

Figure 4.- Sketch of model simulator. All dimensions are in centimeters except where noted.

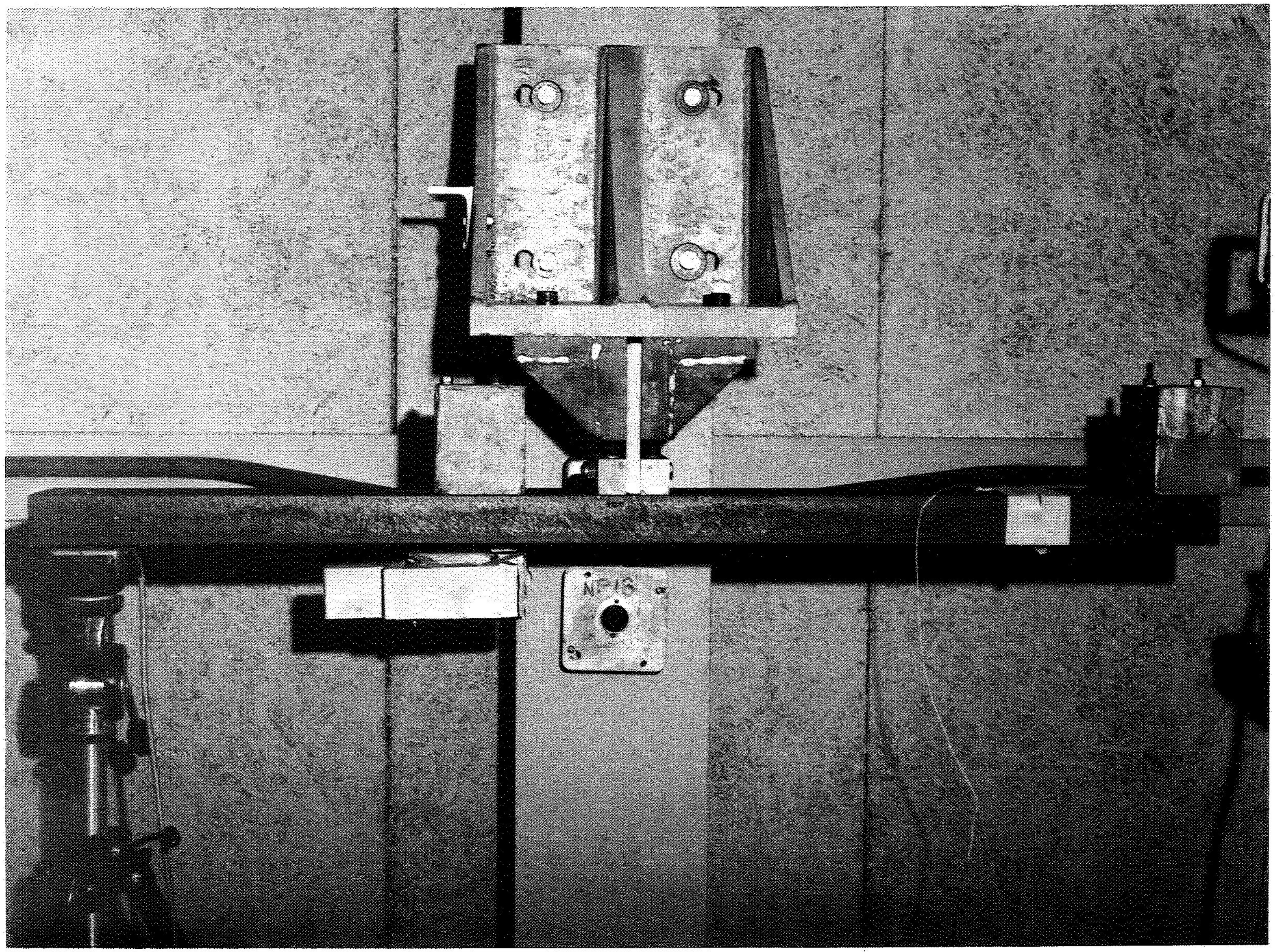

Figure 5.- Photograph of model simulator showing shaker on stand at left.

L-64-10,133

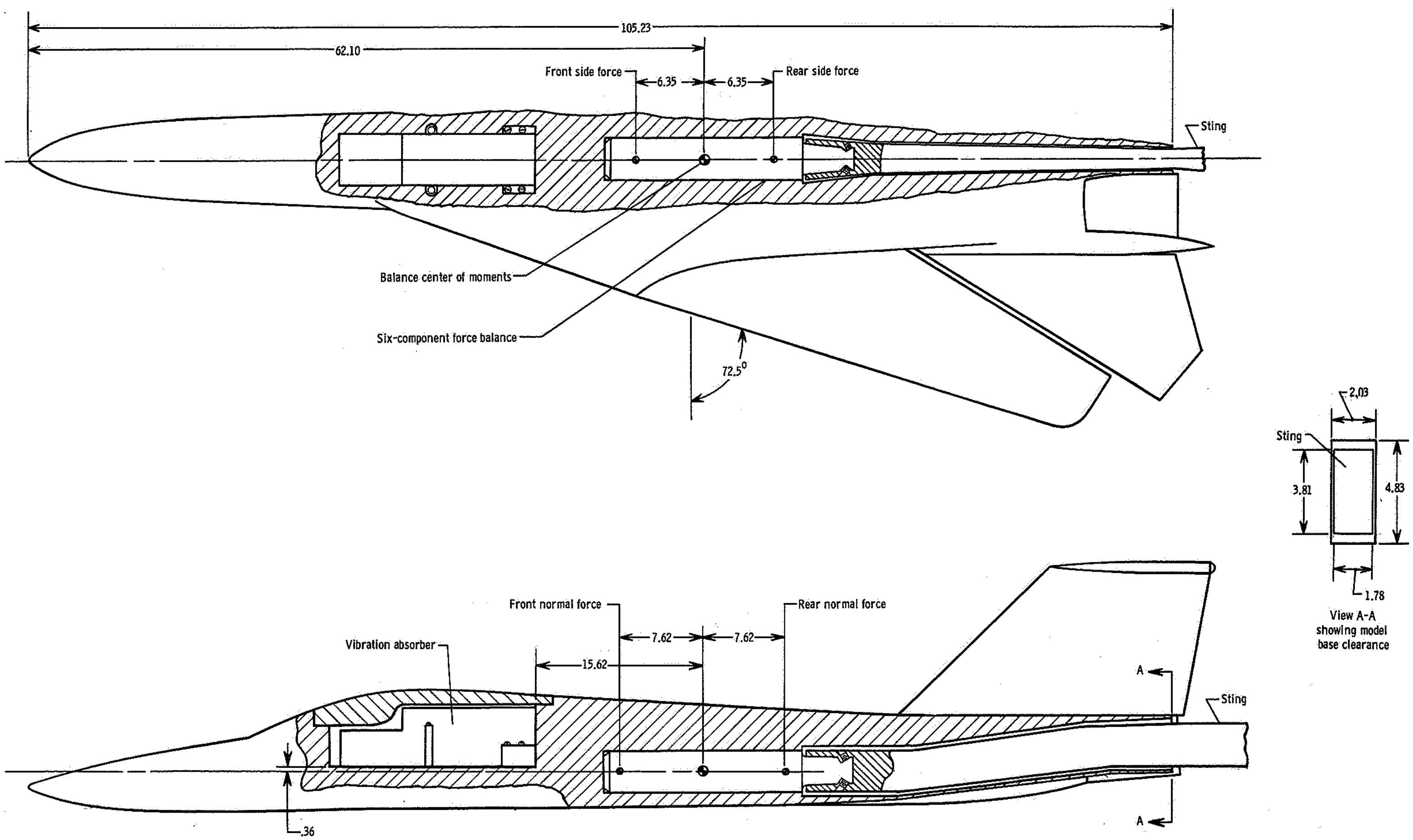

Figure 6.- Sketch of model. All dimensions are in centimeters except where noted.

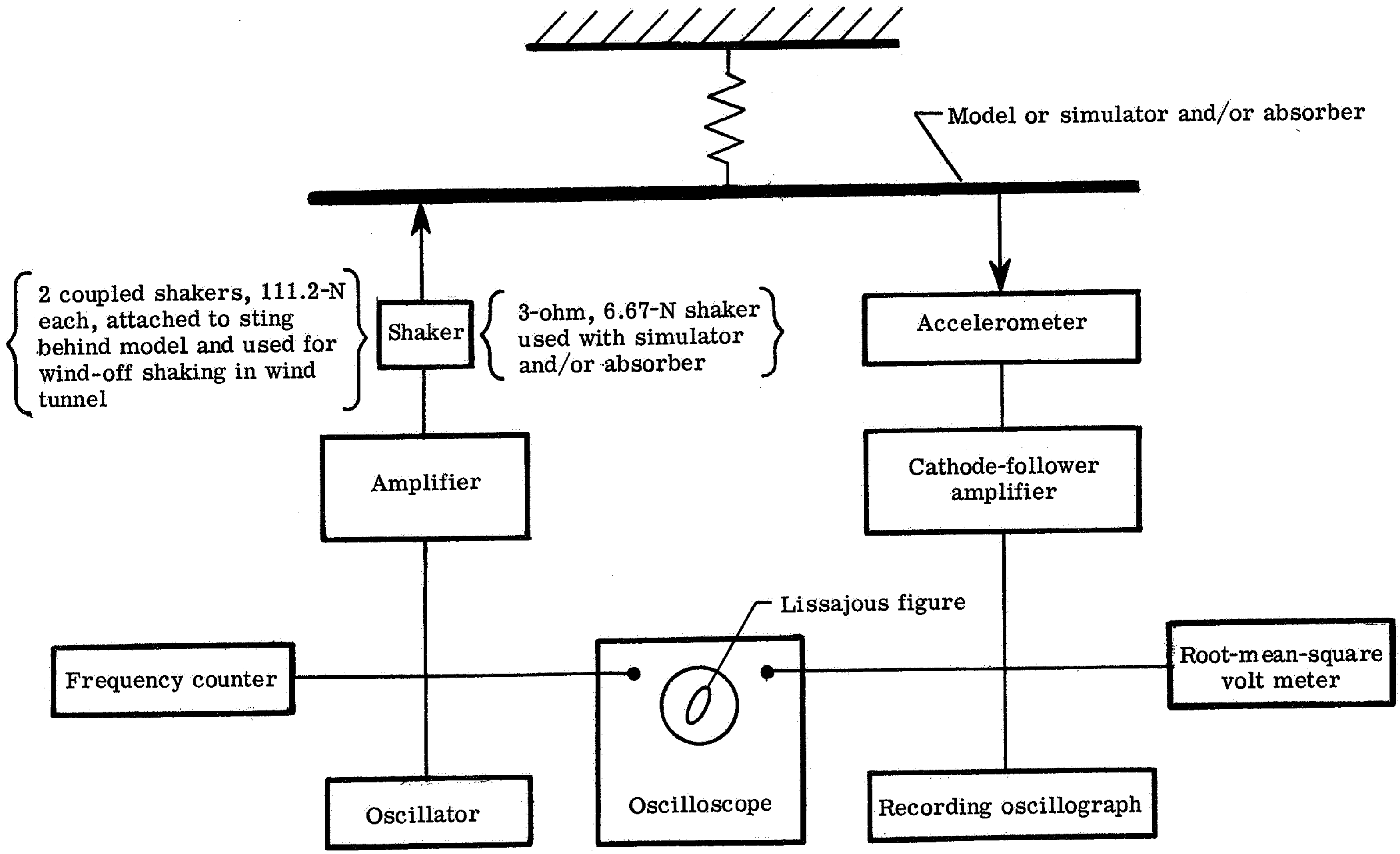

(a) To obtain response curves and model frequencies (wind off).

Figure 7.- Block diagrams of instrumentation used.

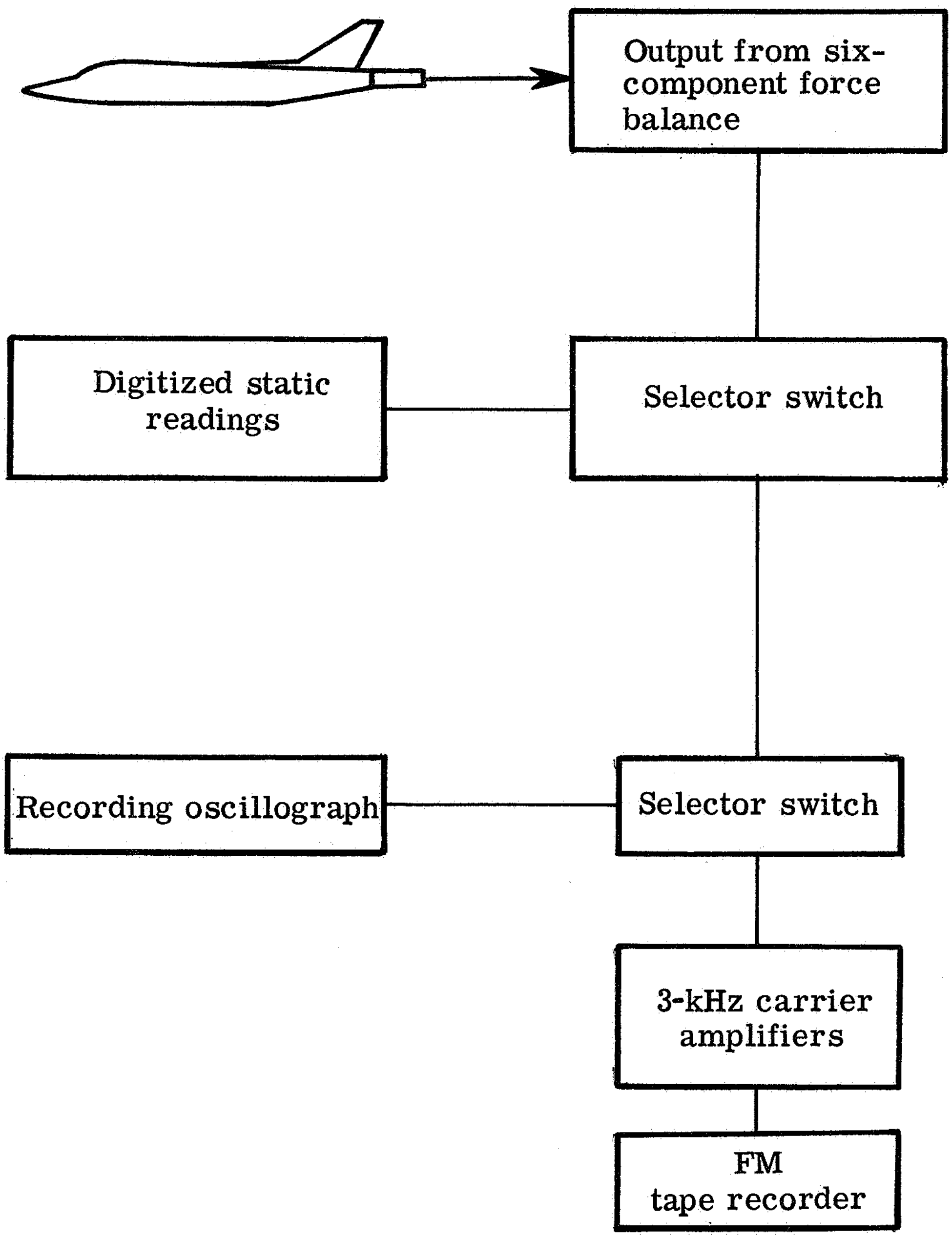

(b) To obtain wind-on force-balance responses.

Figure 7.- Concluded.

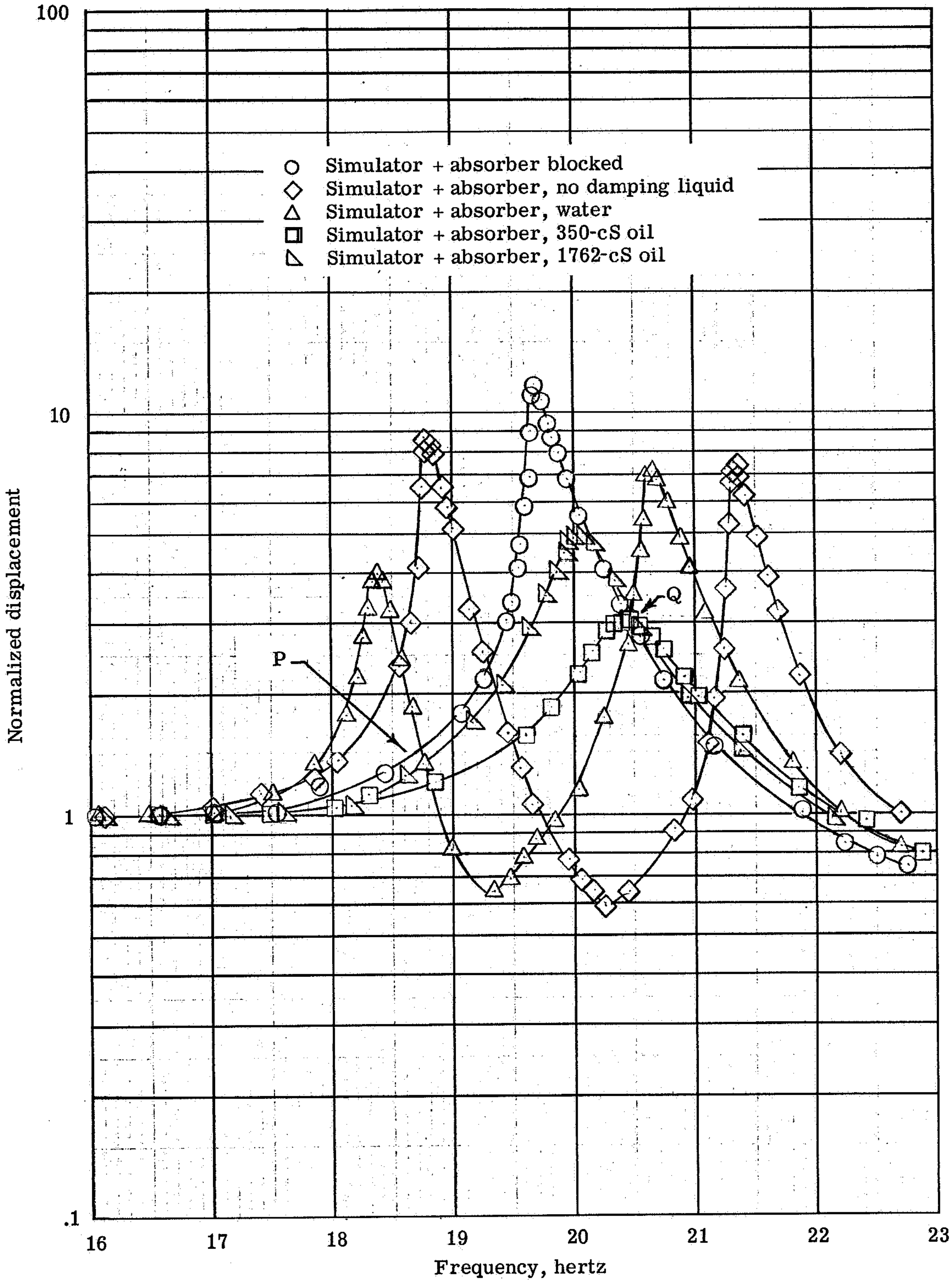

Figure 8.- Effects of various damping fluids on frequency-response characteristics, spring 1, simulator resonant frequency 20.1 hertz, absorber in yaw with mass center 18 cm from effective node.

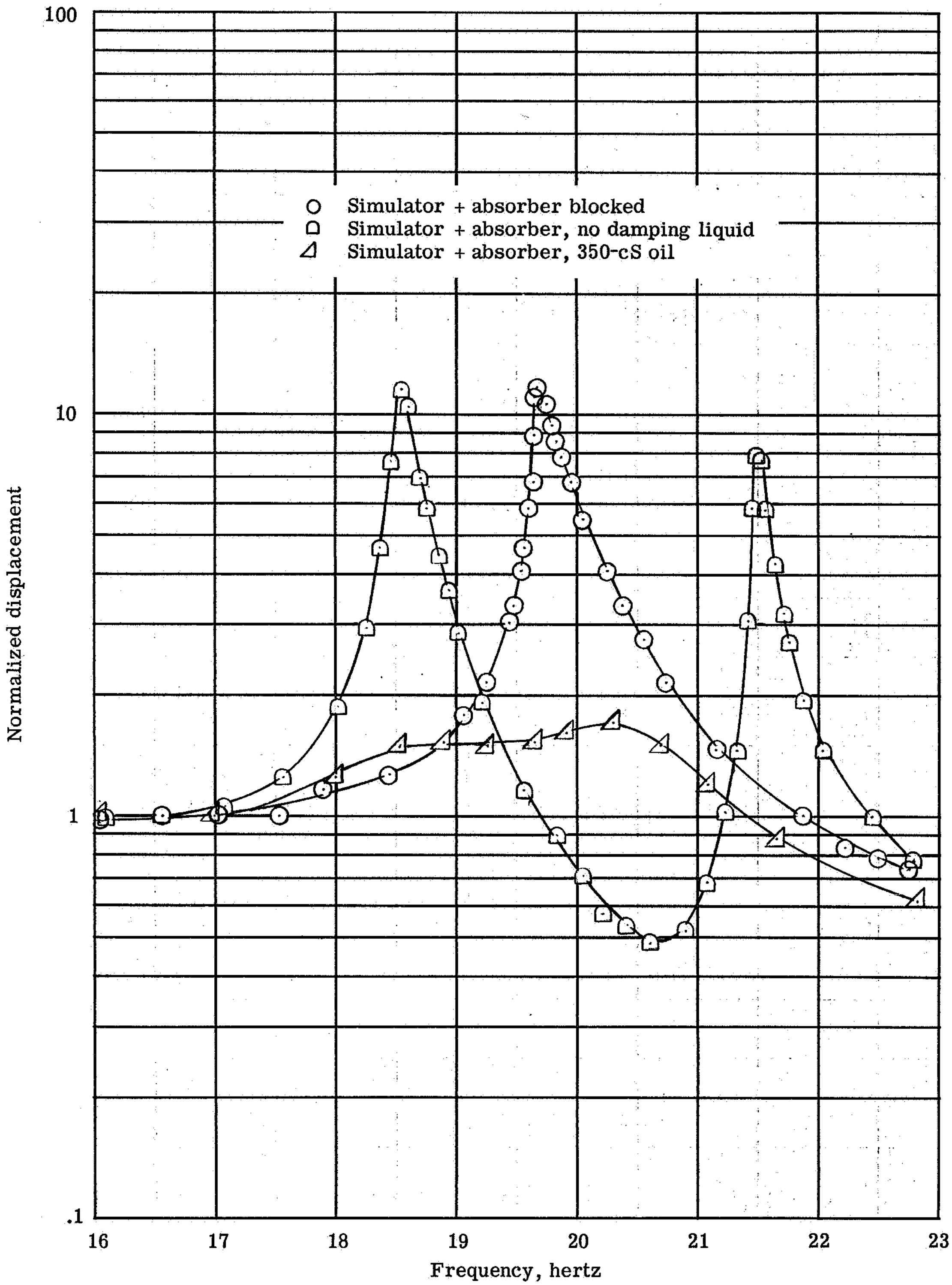

Figure 9.- Frequency-response characteristics for vibration absorber showing results of near-optimum tuning, spring 2, simulator resonant frequency 20.1 hertz, absorber in yaw with mass center 18 cm from effective node.

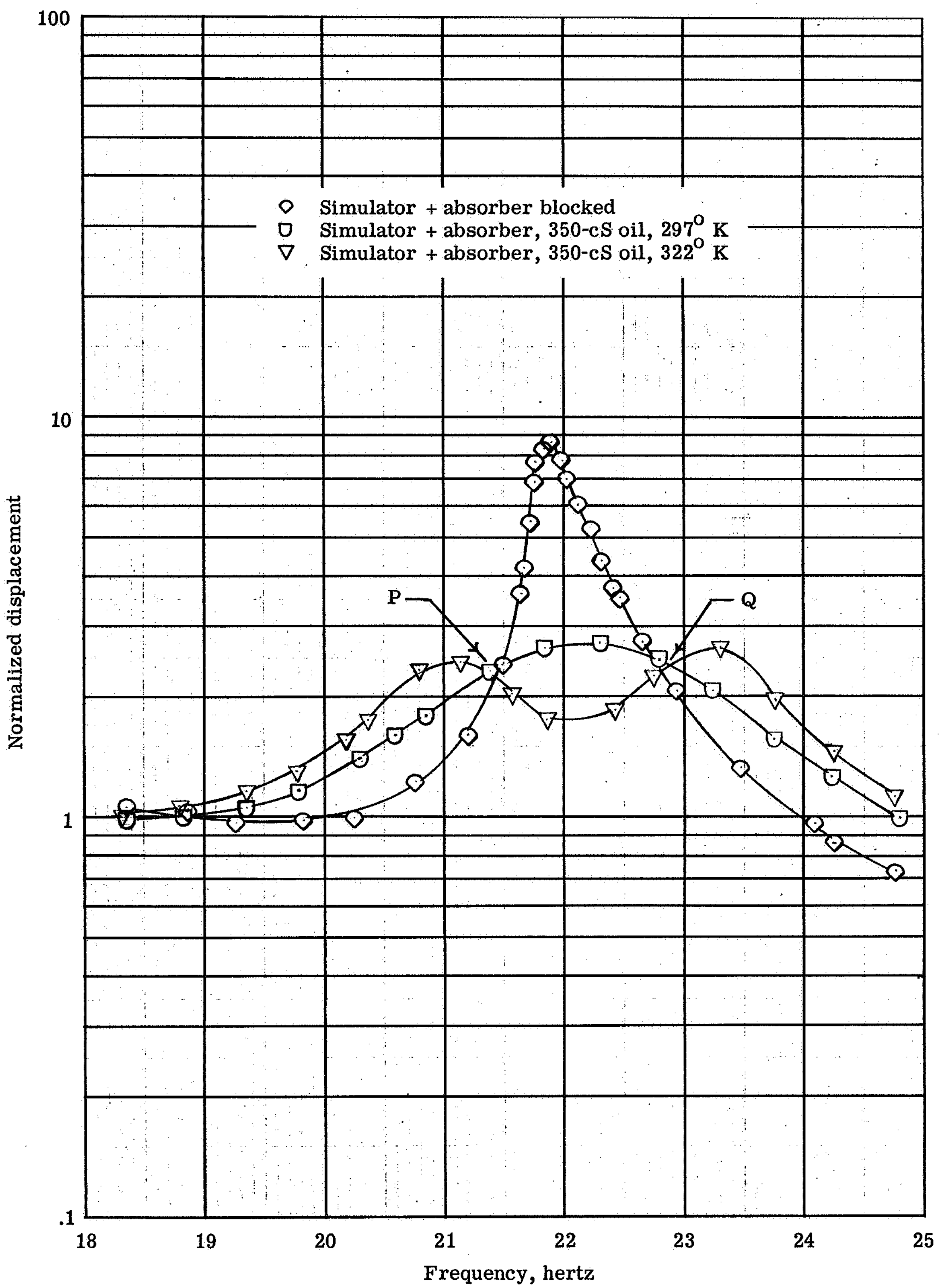

Figure 10.- Effect of oil temperature change on frequency-response characteristics of vibration absorber, spring 4, simulator resonant frequency 22.5 hertz, absorber in yaw with mass center 18 cm from effective node.

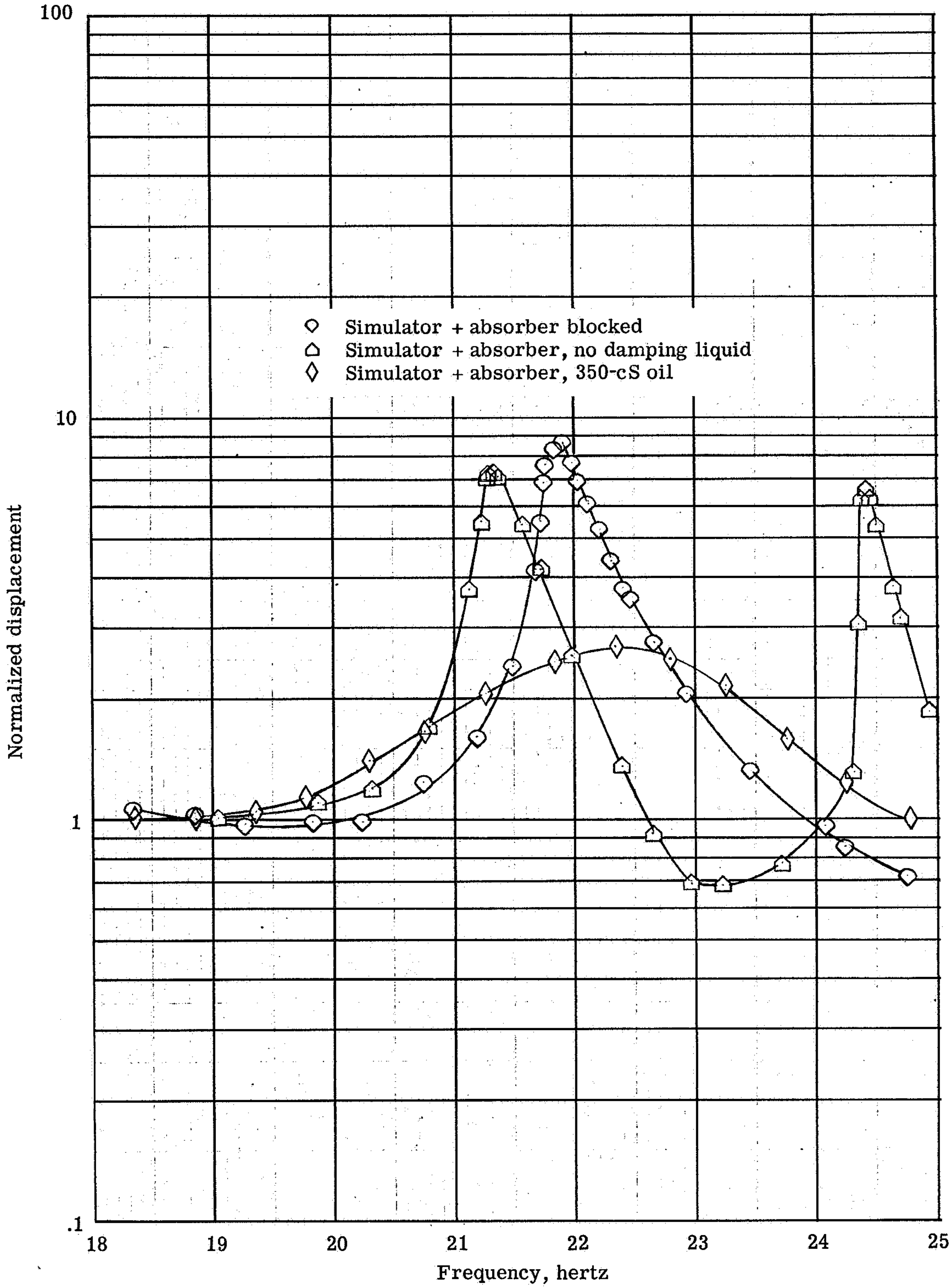

Figure 11.- Frequency-response characteristics of vibration absorber in yaw, spring 3, simulator resonant frequency 22.5 hertz, absorber mass center 18 cm from effective node.

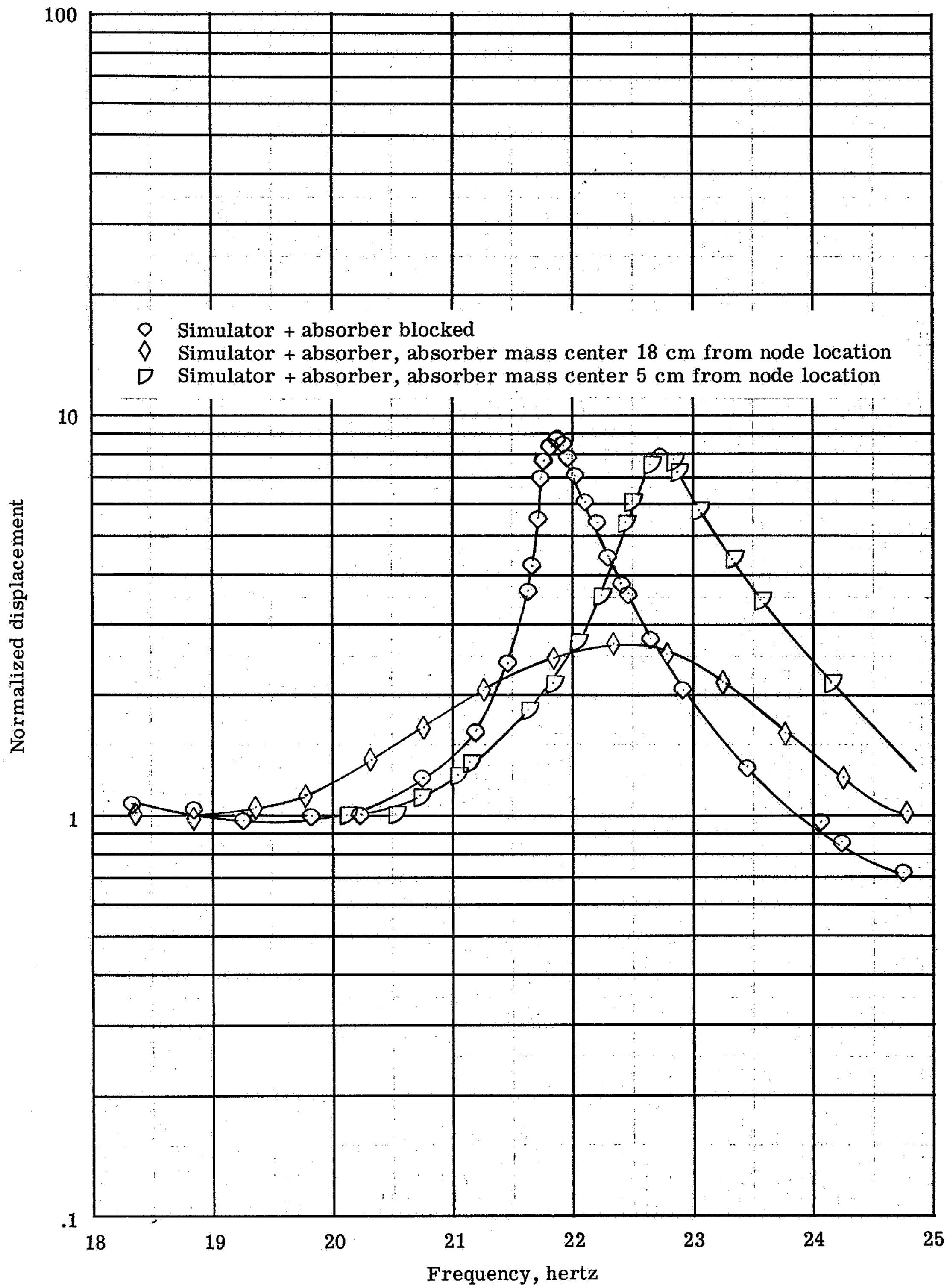

Figure 12.- Frequency-response characteristics in yaw for two vibration-absorber positions, spring 3, 350-cS oil, simulator resonant frequency 22.5 hertz.

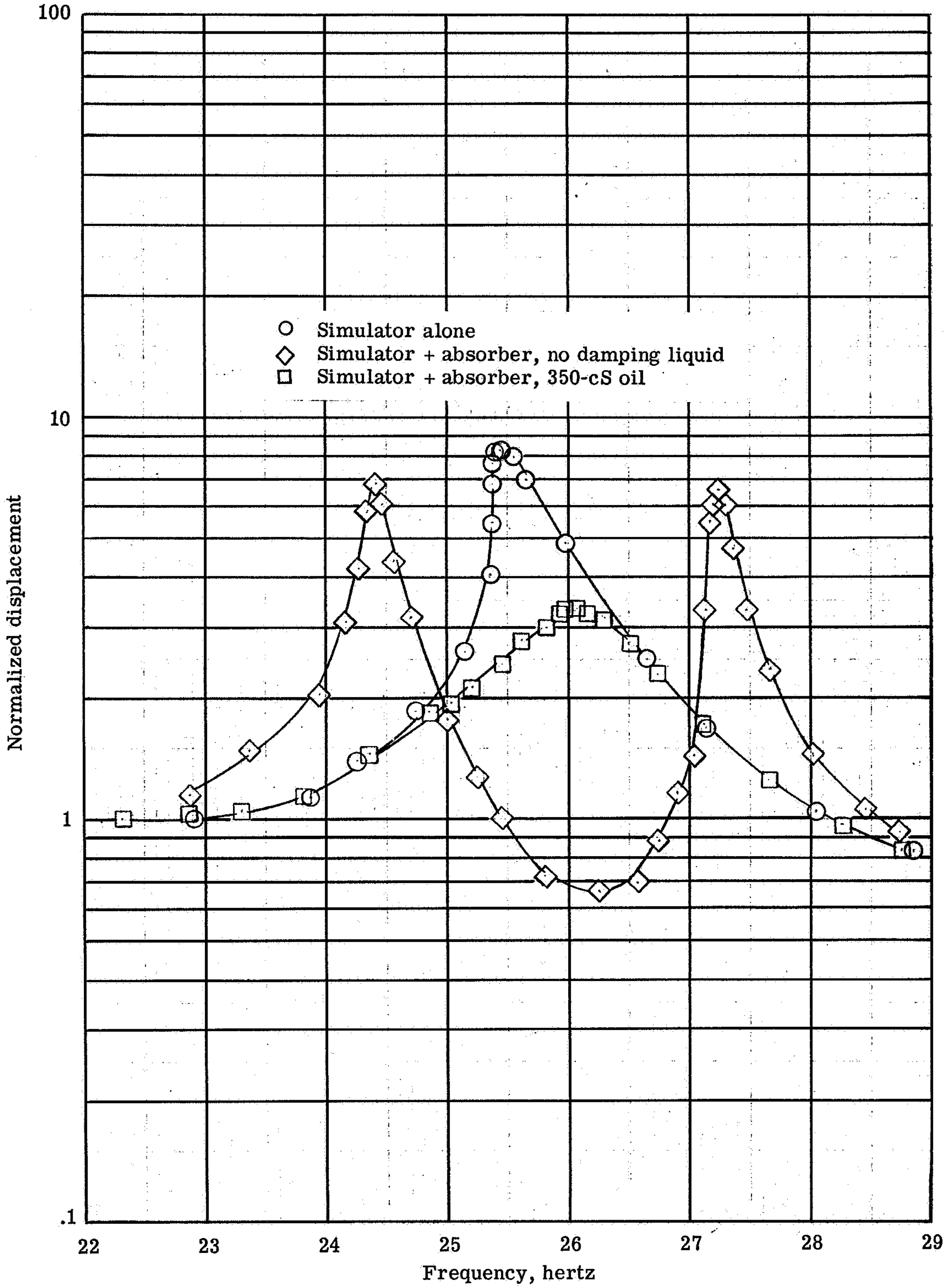

Figure 13.- Frequency-response characteristics for vibration absorber in pitch, spring 3, simulator resonant frequency 25.4 hertz, absorber mass center 18 cm from effective node.

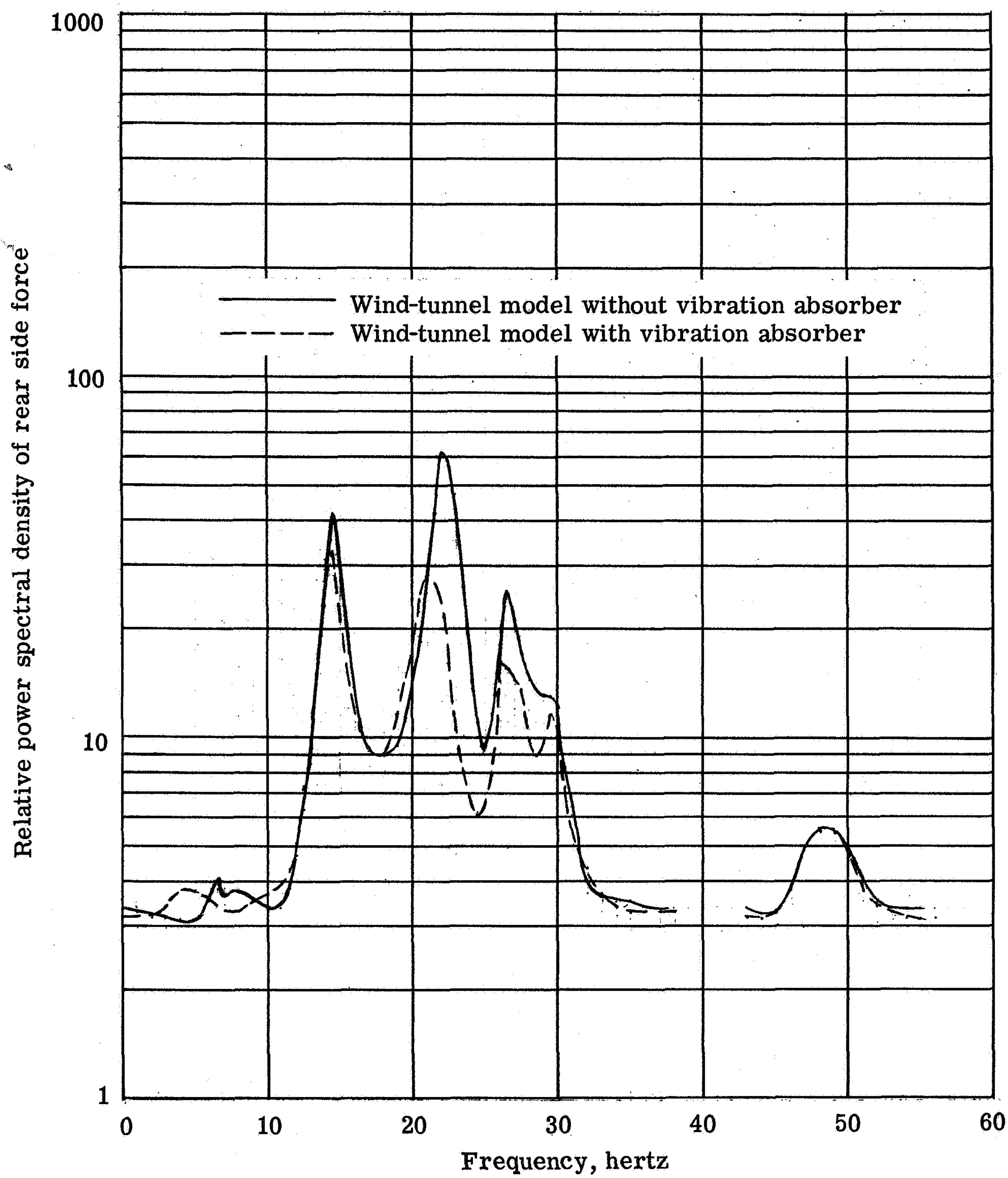

Figure 14.- Relative power spectral density of rear side force for the wind-tunnel model with and without the vibration absorber at a Mach number of 1.16.

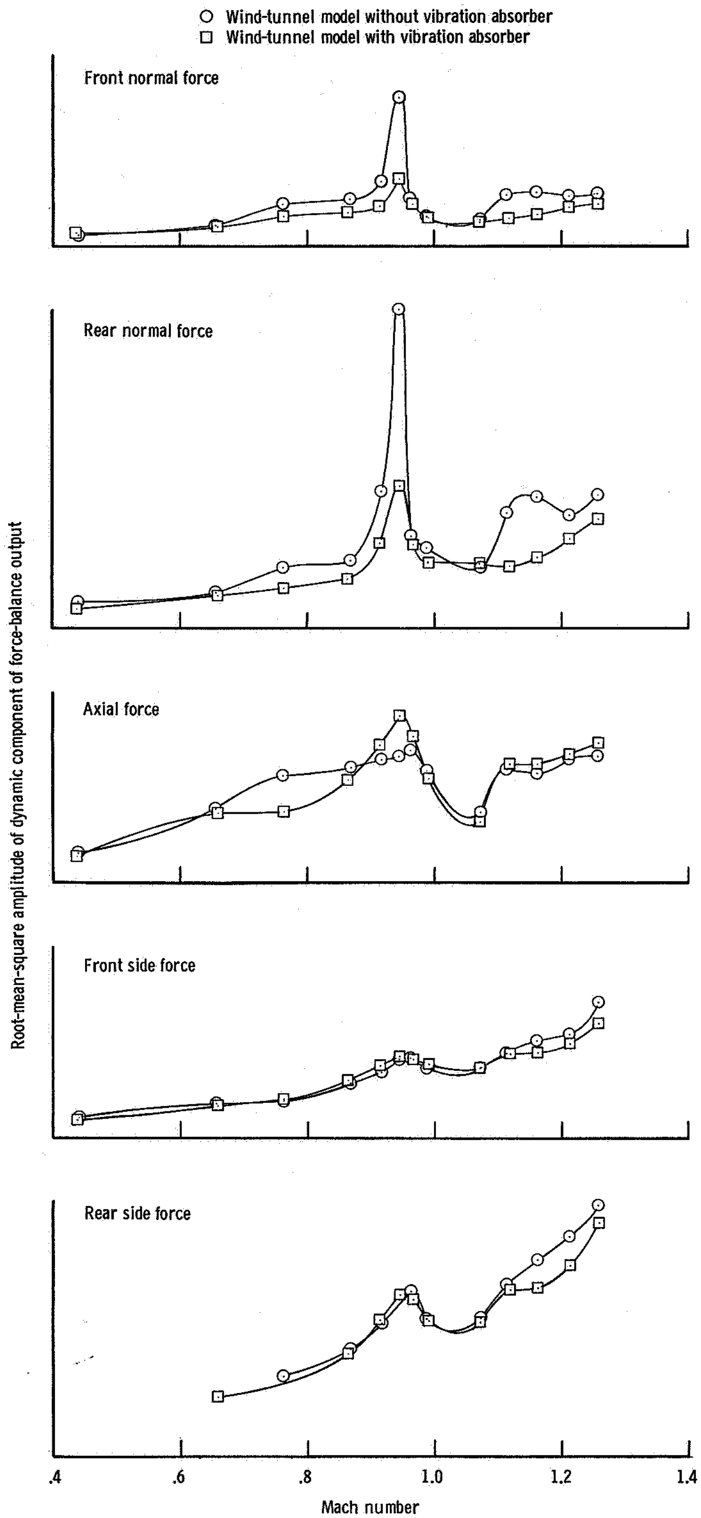

Figure 15.- Variations with Mach number of root-mean-square amplitudes of dynamic components of force-balance output.

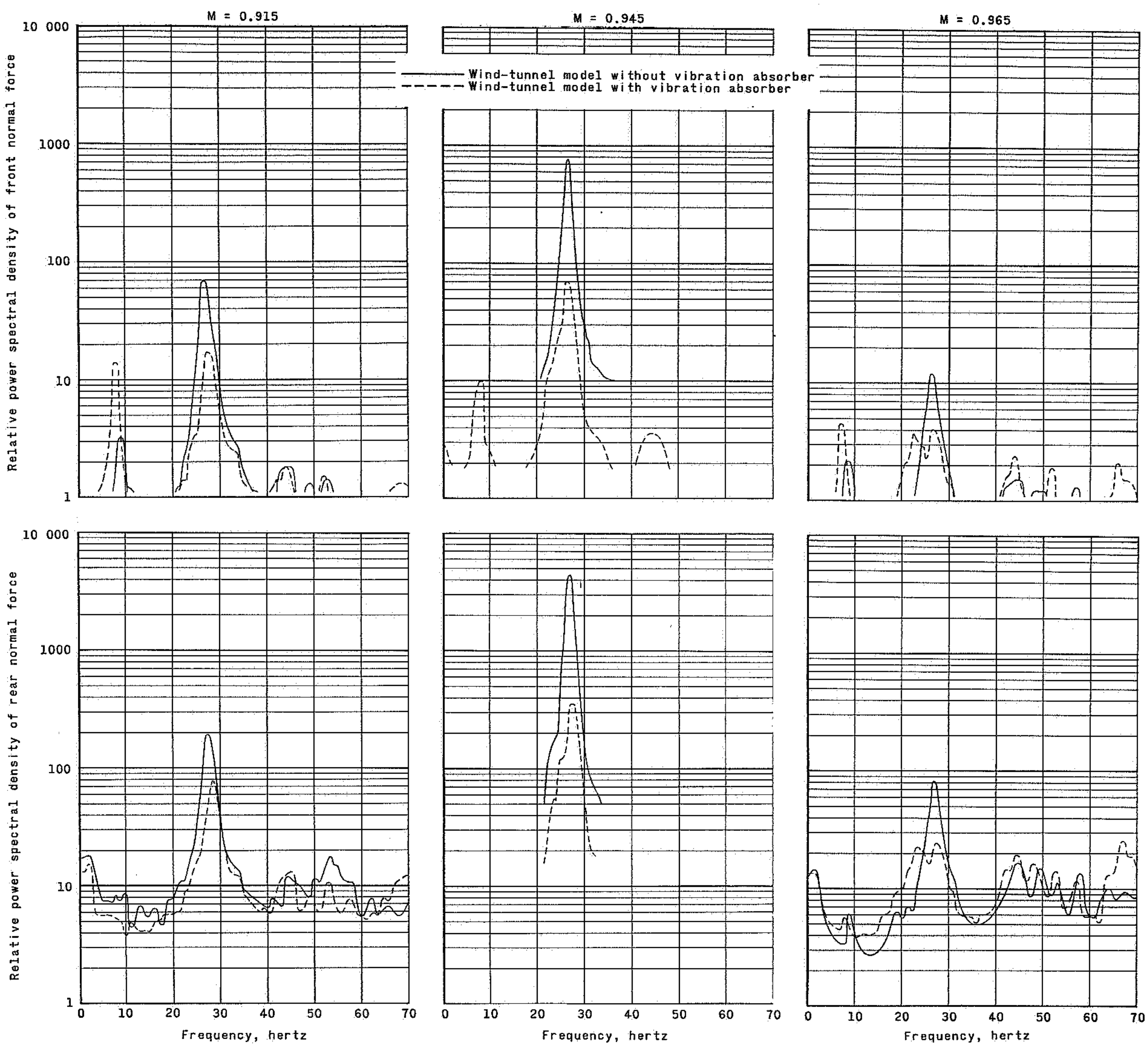

Figure 16.- Relative power spectral densities of front and rear normal forces for the wind-tunnel model with and without the vibration absorber.

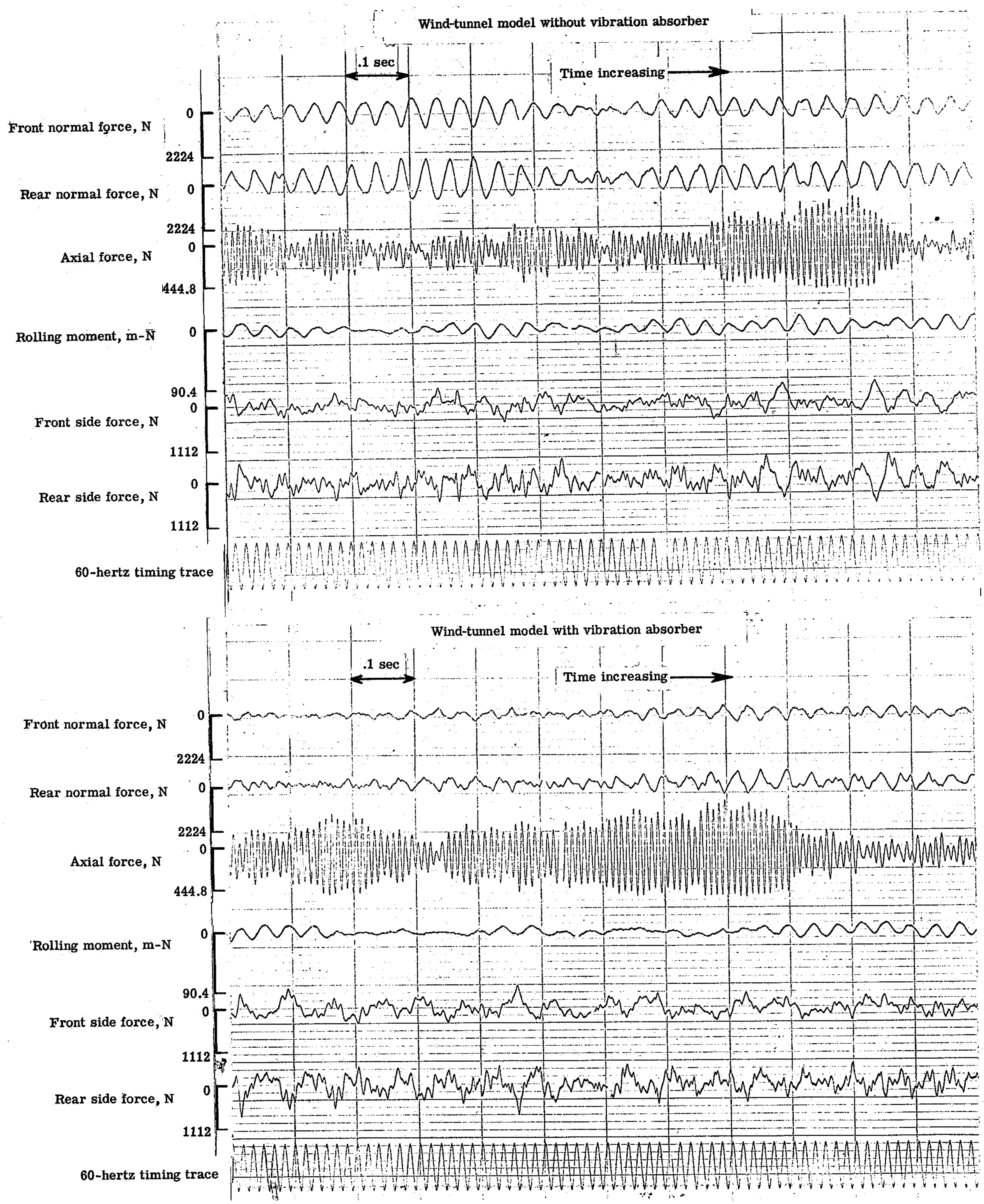

Figure 17.- Time-history oscillograph traces of six-component force-balance outputs at a Mach number of 0.945. Values on scales represent maximum positive balance load limits.

NASA-Langley, 1968 —— 17 L

"The aeronautical and space activities of the United States shall be conducted so as to contribute . . . to the expansion of human knowledge of phenomena in the atmosphere and space. The Administration shall provide for the widest practicable and appropriate dissemination of information concerning its activities and the results thereof."

—NATIONAL AERONAUTICS AND SPACE ACT OF 1958

NASA SCIENTIFIC AND TECHNICAL PUBLICATIONS

TECHNICAL REPORTS: Scientific and technical information considered important, complete, and a lasting contribution to existing knowledge.

TECHNICAL NOTES: Information less broad in scope but nevertheless of importance as a contribution to existing knowledge.

TECHNICAL MEMORANDUMS: Information receiving limited distribution because of preliminary data, security classification, or other reasons.

CONTRACTOR REPORTS: Scientific and technical information generated under a NASA contract or grant and considered an important contribution to existing knowledge.

TECHNICAL TRANSLATIONS: Information published in a foreign language considered to merit NASA distribution in English.

SPECIAL PUBLICATIONS: Information derived from or of value to NASA activities. Publications include conference proceedings, monographs, data compilations, handbooks, sourcebooks, and special bibliographies.

TECHNOLOGY UTILIZATION PUBLICATIONS: Information on technology used by NASA that may be of particular interest in commercial and other non-aerospace applications. Publications include Tech Briefs, Technology Utilization Reports and Notes, and Technology Surveys.

Details on the availability of these publications may be obtained from:

SCIENTIFIC AND TECHNICAL INFORMATION DIVISION

NATIONAL AERONAUTICS AND SPACE ADMINISTRATION

Washington, D.C. 20546